Vol 16 No 5, May 2007
1009-1963/2007/16(05)/1374-11

Chinese Physics

© 2007 Chin. Phys. Soc.
and IOP Publishing Ltd

Decreased vibrational susceptibility of Fabry–Perot cavities via designs of geometry and structural support*

Yang Tao(杨 涛)[a], Li Wen-Bo(李文博)[a], Zang Er-Jun(臧二军)[b], and Chen Li-Sheng(陈李生)[c]†

[a] *Department of Physics, Beijing Jiaotong University, Beijing* 100044, *China*
[b] *National Institute of Metrology, Beijing* 100013, *China*
[c] *Wuhan Institute of Physics and Mathematics, Chinese Academy of Sciences, Wuhan* 430071, *China*

(Received 9 July 2006; revised manuscript received 28 November 2006)

Ultra-stable optical cavities are widely used for laser frequency stabilization. In these experiments the laser performance relies on the length stability of the Fabry–Perot cavities. Vibration-induced deformation is one of the dominant factors that affect the stability of ultra-stable optical cavities. We have quantitatively analysed the elastic deformation of Fabry–Perot cavities with various shapes and mounting configurations. Our numerical result facilitates a novel approach for the design of ultra-stable cavities that are insensitive to vibrational perturbations. This approach can be applied to many experiments such as laser frequency stabilization, high-precision laser spectroscopy, and optical frequency standards.

Keywords: optical cavity, laser frequency stabilization, optical frequency standard, precision measurement
PACC: 4260D, 0765, 4262E, 4260

1. Introduction

A Fabry–Perot cavity can serve as a frequency reference onto which the frequencies of several types of lasers are locked with high precision.[1,2] These lasers are widely used in the fields of optical frequency standards, measurements of fundamental constants, high-resolution spectroscopy, and tests of fundamental physics.[3–9] In the literature the well-isolated and high-finesse Fabry–Perot cavity is often referred to as ultra-stable cavities. Figure 1 sketches a typical configuration of Fabry–Perot cavities. Usually, an ultra-stable cavity consists of two high-reflection mirrors situated face to face with each other and aligned with the optical axis.[10,11] The two mirrors are sandwiched by a spacer that is made of materials with low coefficient of thermal expansion (CTE) such as ULE and Zerodur. The substrates of mirrors are frequently made of the same material as that of the spacer and are optically contacted onto the end of the spacer. Reflective index of the air between the two mirrors varies with the temperature, pressure, and humidity which are constantly undergoing fluctuations. Thus the fluctuation of the air reflective index modifies the optical length between the two mirrors, and hence the cavity has to be placed in a vacuum chamber. In addition, to cope with the ambient temperature drift and the seismic vibration, the vacuum chamber is temperature-controlled within a few tens of millikelvin and is mounted on some vibration-isolated platform.[2]

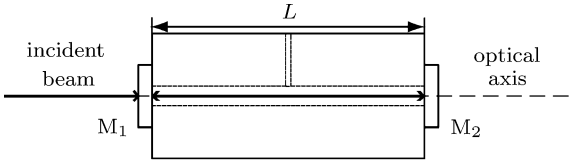


Fig.1. Basic configuration of a Fabry–Perot cavity. The cavity consists of two high-reflection mirrors sandwiched by a cavity spacer. A centre hole is bored through the whole length of the spacer. A side hole is used for the evacuation of the air trapped in the centre hole. Vibrations induce the deformation of the cavity, resulting in a change of the cavity length, ΔL. The vibration-induced cavity deformation constantly varies the length of the cavity, which in turn modulates the frequency of the laser that is locked to the cavity. M_1: input mirror. M_2: output mirror. L: The optical length of the cavity.

In experiments where the lasers are referenced to Fabry–Perot cavities, the optical frequency drift is induced by the change of optical length between two

*Project supported by National Institute of Metrology and Wuhan Institute of Physics and Mathematics, Chinese Academy of Sciences.
†E-mail: lchen@wipm.ac.cn

mirrors.[12] Environmental vibrational perturbations evoke elastic deformations of the cavity, which in turn change the optical length of the cavity. Under vibrational perturbations, the two mirrors are not only deformed but also tilted because of the bending of the spacer. Therefore, the deformation of the spacer greatly affects the stability of the cavity on which the laser frequency is referenced. Indeed, great efforts have been made to attenuate the vibrations that seriously undermine the length stability of the cavity.

However, to the best of our knowledge, a quantitative investigation of the elastic deformation of ultra-stable cavities has not been available. Two approaches usually employed in the traditional vibration control are the passive isolation and the active cancellation. In the passive mode cavities are mounted on vibration damping materials like springs or soft cushions, or suspended by vertical strands of surgical tubing,[2] while the active vibration control uses a certain type of actuator [such as piezoelectric transducers (PZTs)] to actively control the movement of the platform. In traditional vibration control most high-frequency components of the vibration are filtered out, but it is a great technical challenge to achieve enough attenuations ($>$ 20 dB) at low frequencies. Most of these damping equipments also exhibit resonant frequencies, though they can be designed to be as small as several hertz by modifying the structures and selecting the materials for these vibration isolations. Presently, with relatively high cost resonant frequencies can be reduced to a few hertz in well-designed passive vibration control and in most of active models. Unfortunately, below these resonant frequencies vibrations transmit freely through the isolation stage. Even worse, if the damping is insufficient near the resonant frequency, vibrations will be enhanced, instead of being attenuated.

In this paper we introduce a novel approach[13] different in principle from the traditional vibration control.[2] We modify the shapes and the mounting configurations of ultra-stable cavities in a special way such that the critical dimensions of the cavities are insensitive to the vibration-induced deformation below 10 Hz (note that the deformation always exists whenever there are vibrational perturbations.) The numerical results given here validate this approach for the vibration control and provide a useful guidance for the cavity design. Various cavity geometries and the related mounting configurations obtained in our numerical modelling can be used in the development of high precision time and frequency standards and in the tests of fundamental laws of physics.

We organize the paper as follows. In Section 2 we introduce the numerical method used to calculate the elastic deformation of the cavity. Terminologies relevant to the numerical analysis such as the displacement and the strain of the mirror are also introduced in this section. Section 3 presents the numerical results for several cavities with different shapes and mounting configurations. The vibration sensitivity of these cavities is quantitatively analysed and several stable numerical models are identified. Considering that many factors could potentially affect the accuracy of the modelling, we discuss the precision of the numerical analysis in Section 4. Section 5 summarizes the analysis.

2. Methods of numerical modelling

Figure 2 illustrates the displacement and the strain of an elastic solid undergoing a certain amount of deformation. Points A and B represent two points in the solid object. Before deformation, the distance between A and B is d and the location of A can be described by a vector $\boldsymbol{r}$. When the deformation happens, points A and B are displaced, as depicted in Fig.2. The displacement of point A is expressed as $\boldsymbol{l} = \boldsymbol{r}' - \boldsymbol{r}$. As the object is deformed, d changes to d' and the fractional change in d describes the local strain in the solid, thus the deformation of a system can be obtained from the displacements of all the points involved in the system.

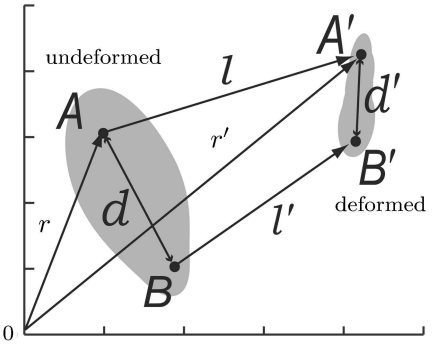


Fig.2. Displacement and strain in an elastic solid. A and B denote two points in the solid without deformation. After deformation, point A is displaced to A', and B to B'. $\boldsymbol{l}$ and $\boldsymbol{l}'$ are the displacements of points A and B respectively. Because of deformation, the distance between A and B is also changed. The strain is defined as the fractional change of an infinitesimal distance after the deformation.

In numerical models, the displacement of each mirror is determined from the probe points locating on the inner surface of the mirror and covering the whole diameter of the through hole as shown in Fig.3(c). The change in cavity length ΔL can be determined from the differential displacement of the two mirrors. We focus on ΔL in our numerical analysis because L is a critical dimension that induces the frequency noise of the laser referenced to the cavity.

The time-dependent vibration poses a technical challenge to the quantitative analysis of the cavity deformation because the spectrum of the vibration covers a wide band and because of the random character of the vibration. However, most high-frequency vibrations can be attenuated by the traditional vibration control. As a result, the Fourier frequencies in the unattenuated vibration spectrum are much lower than the eigenfrequencies of the cavity. If the support is fixed, its acceleration caused by the vibration can be replaced by a force of gravity applied to the cavity, and the direction of the gravity is opposite to that of the vibrational acceleration. Thus the dynamic problem is reduced to a static analysis. We use Cosmosworks and ANSYS, two finite element analysis (FEA) packages, to evaluate the elastic deformation of the cavities under the influence of a simulated gravity.

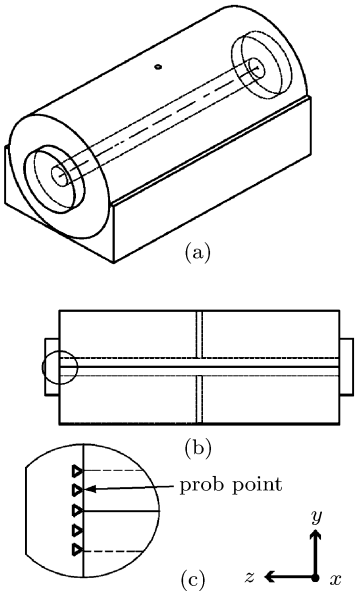


Fig.3. Cylindrical cavity on a U-shaped block. Cylindrical cavity on a U-shaped block is one of the common configurations in laser frequency stabilization. (a) 3D view of the cavity. (b) An axial cross section of the cavity. (c) Details of the probe points on the inner surface of the mirror. Probe points are placed on the inner surface of the mirror to cover the whole transverse area of the through hole.

3. Numerical results for cavities with various geometries and mounting configurations

In this section we numerically model several types of cavities that are frequently used in laser frequency stabilization. We modify the shapes and mounting configurations of these cavities to find the critical point at which the variations of the optical length induced by vibrations can be minimized and the surfaces of the two mirrors are parallel to each other. We have identified this critical point for various cavity geometries and mounting methods.

3.1. Cylindrical cavities with horizontal mounting

Figure 3(b) shows a cylindrical cavity mounted on a U-shaped block. We place several probe points on the inner surface of each mirror, as illustrated in Fig.3(c). A force of gravity is applied downward, denoted by $g < 0$. Figure 4(a) shows the strain distribution in an axial cross section and the amplified ($\times 10^5$) cavity deformation. The cavity is compressed along the $-y$ direction and elongated in the z direction. To focus on the change of the optical length, Fig.4(c) shows the displacements of the two mirrors at the locations of probe points. Again, the displacements of the two mirrors can be qualitatively inferred from Fig.4(a). The left mirror moves along the z-axis and the right mirror moves in the reverse direction. The cavity is elongated, defined as $\Delta L > 0$. The magnitude of ΔL is 1.6×10^{-10} m as shown in Fig.4(c).

Changing the direction of the gravity and repeating the numerical calculation, we observe that the cavity is stretched along the y axis and shortened along the z axis, as shown in Fig.4(b). Compared with the case of a downward gravity, ΔL, the change of the cavity length, reverses its sign, but keeps its magnitude. The left mirror moves along the $-z$ direction and the right one shifts towards the opposite direction, while the two mirrors are approximately parallel to each other, as shown in Fig.4(d).

The U-block mounting method has been widely adopted in various experiments, as part of the traditional vibration control. According to our numerical modelling, however, this configuration allows for a change of cavity length induced by the instantaneous vibrational acceleration. As discussed in the introduction, low-frequency components of the vibration can-

not be efficiently attenuated by the damping materials inserted between the U block and the optical platform. As a result, the low-frequency vibrations directly act on the cavity and hence cause the cavity instability. In short, when the cavity is horizontally mounted on a U block, the effectiveness of the traditional vibration control is compromised at low vibration frequencies.

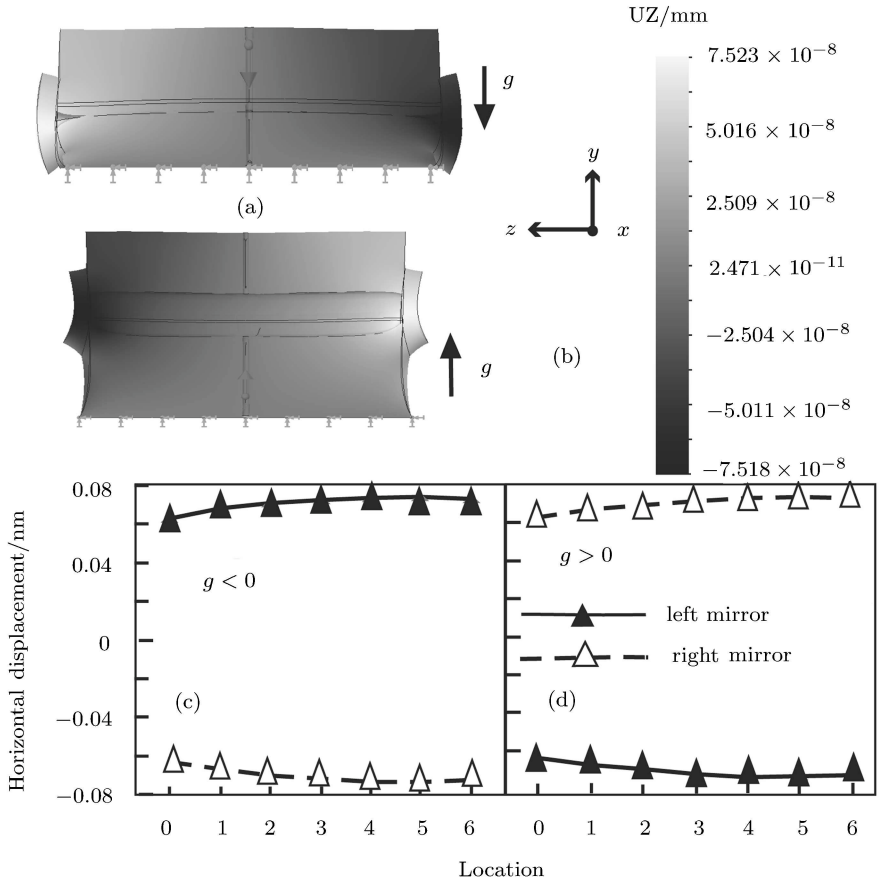


Fig.4. Cylindrical cavity on a U-block. (a) and (b) are the strain distributions in an axial cross section with the gravity applied downward ($-y$) and upward (y), respectively. Note that the deformation of the cavity is amplified force of by a factor of 10^5. (c) and (d) are corresponding mirror displacements with the gravity applied downward and upward.

3.2. Cuboid cavity supported by double beams

We introduce a new mounting scheme to reduce the sensitivity of the cavity to the vibrational perturbation. In this model a long cuboid cavity (270 mm) is mounted on two beams with rectangular cross section, as shown in Fig.5(a). Compared with previous U-block mounting that has no parameter to adjust the supporting position, current configuration has three parameters to be modified, namely the width w, height h, and location d of the beam, as shown in Fig.5(b). The length of the cavity is 270 mm and the two supporting beams are placed on a flat baseplate. Figures 5(c), 5(d), and 5(e) show strain distributions of the cavity. In general, the strain distribution inside the cavity varies with the change of d, i.e., the position of the structural support. Less obvious is the supporting position and the area of the contacting surface that also affect the length of the cavity. This subtle effect is revealed by our numerical calculations and will be addressed in the following discussion.

To quantitatively investigate how the structural support affects the stability of the cuboid cavity, we adjust three parameters d, w, and h in our numerical analysis. Figure 6 shows the results of this analysis. When w and h are fixed, the two mirrors incline to opposite directions with the same tilting angle. The tilt of the two mirrors evolves with the beam position, as is clearly demonstrated by Figs.6(a), 6(b), and 6(c).

At $d = 20$ mm, the two mirrors incline towards each other, forming a Greek capital letter 'Λ', as indicated in Figs.5(e) and 6(a). When the two beams are moved towards the centre of the spacer, at $d = 30$ mm, their relative orientation can be described by a capital letter 'V', as shown in Figs.5(c) and 6(c). In between two cases, the two mirrors can be brought to positions parallel to each other and this occurs at $d = 26.7$ mm [Figs.5(d) and 6(b)]. This special position for the two supporting beams is called an Airy point.

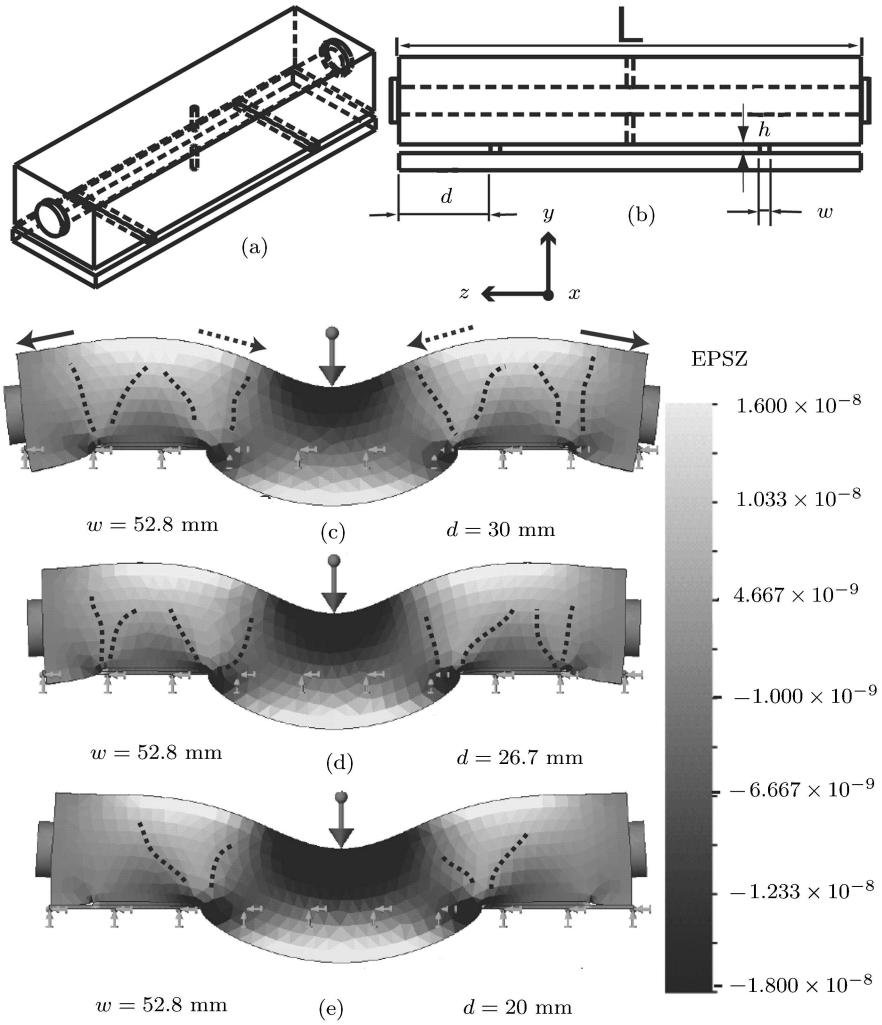


Fig.5. A cuboid cavity supported by double beams. (a) 3D view of the cavity. (b) Right-side view of the cavity. (c), (d), and (e) are the strain distributions in the z direction with the distance d (from the support to the end face of the cavity) = 30, 26.7, and 20 mm, respectively. Note that the width of the supporting beams is fixed to 52.8 mm. A long cavity with a length of 270 mm is used in the numerical modelling. When the gravity is downward, the mirrors rotate around the supporting points, and the whole cavity is compressed along the $-y$ direction and elongated in the z direction.

We then adjust the second parameter, namely the beam width w. To eliminate the mirror tilting, at each w we first vary d to locate the Airy point. A change in cavity length is usually present after this adjustment. Figure 6(e) shows the trend of ΔL in a broad range of w, with the beam height h fixed at 2 mm. Note that the change in cavity length is minimized at $w = 52.8$ mm, indicating a greatly reduced vibrational susceptibility. Above (Below) this point the cavity is elongated (shortened).

For two different values of h, Figs.6(d) and 6(f) again show similar trends of ΔL versus beam width w. As h is varied, the change in cavity length can still be minimized by modifying parameters. For in-

stance, when $h = 1$ mm, the optimized position is found at $d = 28.6$ mm and $w = 52.5$ mm, with $\Delta L = -2 \times 10^{-12}$ mm.

To minimize the vibration sensitivity of the cavity, a general procedure can be drawn from the above discussions. First, the beam position d can be varied to locate the Airy point. When the cavity is supported at Airy point the parallelism of the two mirrors is ensured. Then the beam width can be adjusted to compensate for the change in cavity length. Of course, a coupling exists between these two adjustments. The optimization of cavity design can be achieved by a few rounds of iterative adjustment of d and w.

We have just shown that at a certain supporting position the length of the cavity responds insensitively to vibrations while the two mirrors are parallel to each other, indicating a greatly improved vibration insensitivity of the cavity. In the following discussions we refer to this position as a critical supporting position.

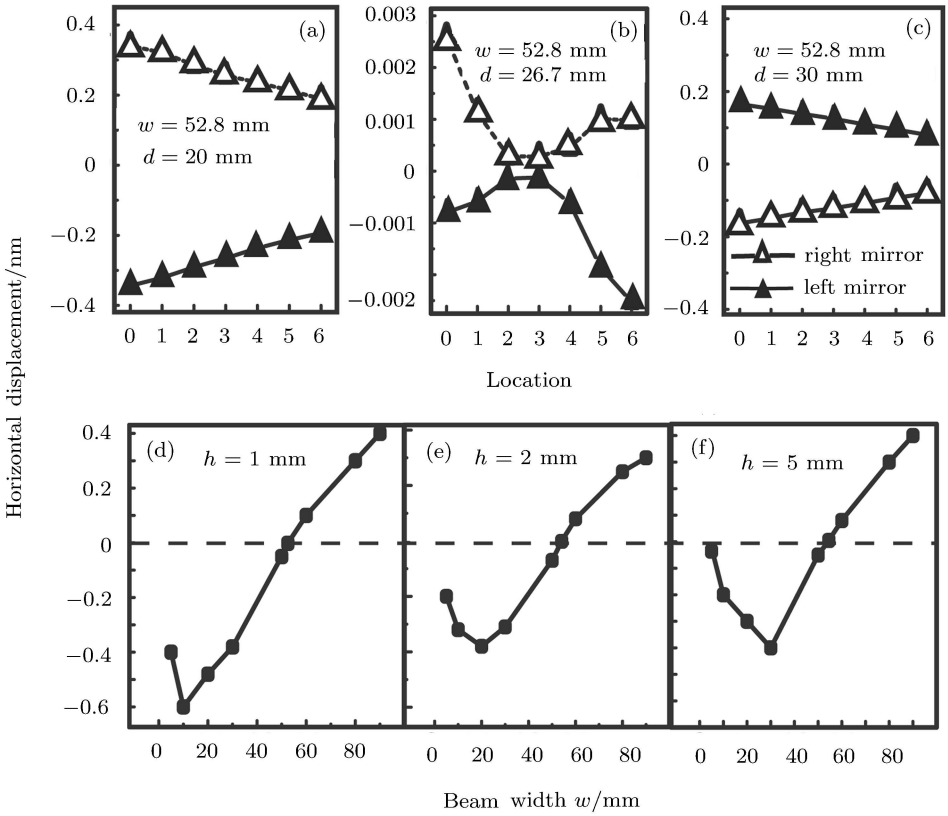


Fig.6. Mirror displacements of the cuboid cavity. (a), (b), and (c) are the displacements of the two mirrors with various d and w when h is fixed at 2 mm. The bottom panels show the change of the optical length at the Airy point as the values of d and w are varied in broad ranges. When h is fixed at 2 mm, the critical point can be located by adjustments of d and w. For a different h, the corresponding critical point can also be found with modified d and w.

3.3. Cuboid cavity supported by four posts

Although we found the critical supporting position for a long (270 mm) cuboid cavity in the preceding section, the related mounting configuration has a limitation. In long cavities a proper bending of the cavity can reduce the effect of the cavity elongation evoked by a gravity-induced vertical compression, resulting in a cavity length that is insensitive to the vibrational perturbation. However, such a preferred supporting position may not be available in a short cavity. Here we introduce an alternative mounting method that can achieve the same vibration insensitivity and also can be implemented in cavities with various dimensions.

Figure 7(a) shows a cuboid cavity supported by four posts. There are several parameters in this

mounting configuration that can be modified, as shown in Fig.7(b). By properly choosing the values of h and d, we obtain the critical supporting position for this model. The relative tilting angle of the two mirrors depends directly on the parameter d, while the cavity length is affected by the hole depth h. Definitely, there are couplings between these two processes. To optimize the supporting position, we iteratively adjust the values of h and d in our calculation to find the critical supporting position at which the vibration sensitivity of the cavity length is minimized and the parallelism of the two mirrors are obtained.

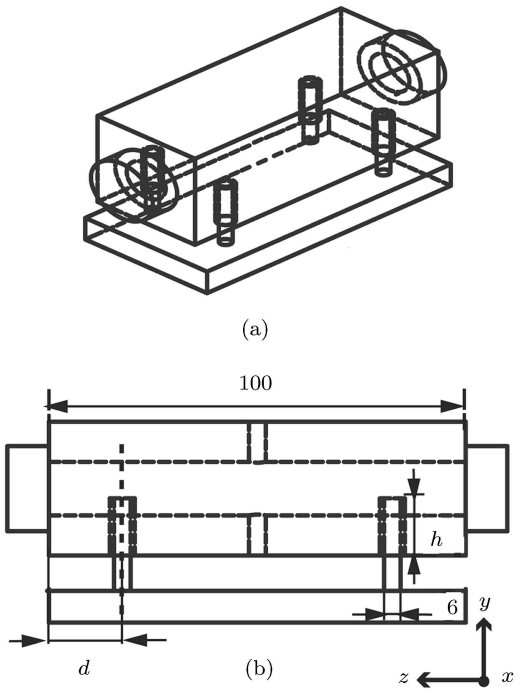


Fig.7. A cuboid cavity supported by four posts. (a) 3D view of the cavity. (b) Side view of the cavity. The length of the cavity is 100 mm, h is the depth of the supporting holes, and d is the distance from the centre of the supporting hole to one end of the cavity. The diameter of the supporting holes is fixed at 6 mm.

To examine the trend of the cavity deformation in terms of supporting position, we change the locations of the posts (d) while fix the depth of the supporting holes (h). As d changes, the tilting angle of the two mirrors varies in a manner similar to what we observed in the previous model where the cavity is mounted on two beams as shown in the upper panel of Fig.8. When the supporting posts are close to the end of the spacer (for instance, $d = 10$ mm, Fig.8(a)) the two mirrors incline towards each other, forming the Greek letter 'Λ'. As the supporting posts are moved towards the centre of the spacer (see, for example, Fig.8(c), where $d = 40$ mm), the relative orientations of the two mirrors resemble the letter 'V'. The parallelism of the two mirrors is obtained at $d = 17.6$ mm with a stretched cavity ($\Delta L \approx 4 \times 10^{-11}$ m).

The cavity is then optimized by iterative trials of h and d. We vary h to compensate for the change in cavity length while the parallelism of the two mirrors can be maintained by adjusting d. We find the critical point when $h = 17.1$ mm and $d = 17.6$ mm, as shown in the central panel of Fig.8. At this point the length change of the cavity is minimized to $\Delta L \approx 1{\times}10^{-12}$ m.

Unlike the two horizontal mounting configurations discussed previously, here the cavity is supported above its bottom. The part below the supporting height is stretched along the y direction and therefore shortened along the z direction, while the upper part of the cavity is compressed along the y direction and elongated along the z direction. Of course, the cavity is also bent by the gravity, resulting in a deformation that affects both the mirror tilting and the cavity length. However, the mirror tilting can be eliminated by supporting the cavity at the Airy point. Consequently, the cavity can be elongated or shortened, depending on the hole depth and the position of the supporting holes. The above analysis indicates that one can always find the critical supporting position by a proper combination of d and h.

As an important model proposed in this paper, we also analyse the systematic errors that can potentially arise in this model. The stability of the critical supporting position is examined by introducing a series of dimensional modifications to the cavity. At the critical supporting position, the diameter of the through hole along the optical axis is varied by 0.05 mm. After calculation we find no obvious change in cavity length ($\Delta L \approx 1 \times 10^{-12}$ m). Adjusting the size of the ventilation hole (5%) produces a change in $\Delta L \approx 1 \times 10^{-12}$ m. To assess the influence of the machine tolerance on the numerical modelling, a 0.1 mm change is applied to d and h. This dimensional modification induces a variation of ΔL within 2×10^{-12} m, which is still two orders of magnitude smaller than the length instability associated with a horizontal cavity resting on a U-shaped block (see Fig.3(a)).

Furthermore, we also consider the third adjustable parameter, namely the diameter of the supporting post. When we reduce the diameter (6 mm) of the posts by ±1 mm at the critical supporting position, the resultant ΔL is almost five times larger than that of the original configuration. Nevertheless, this change in ΔL can always be compensated by a new adjustment of d and h.

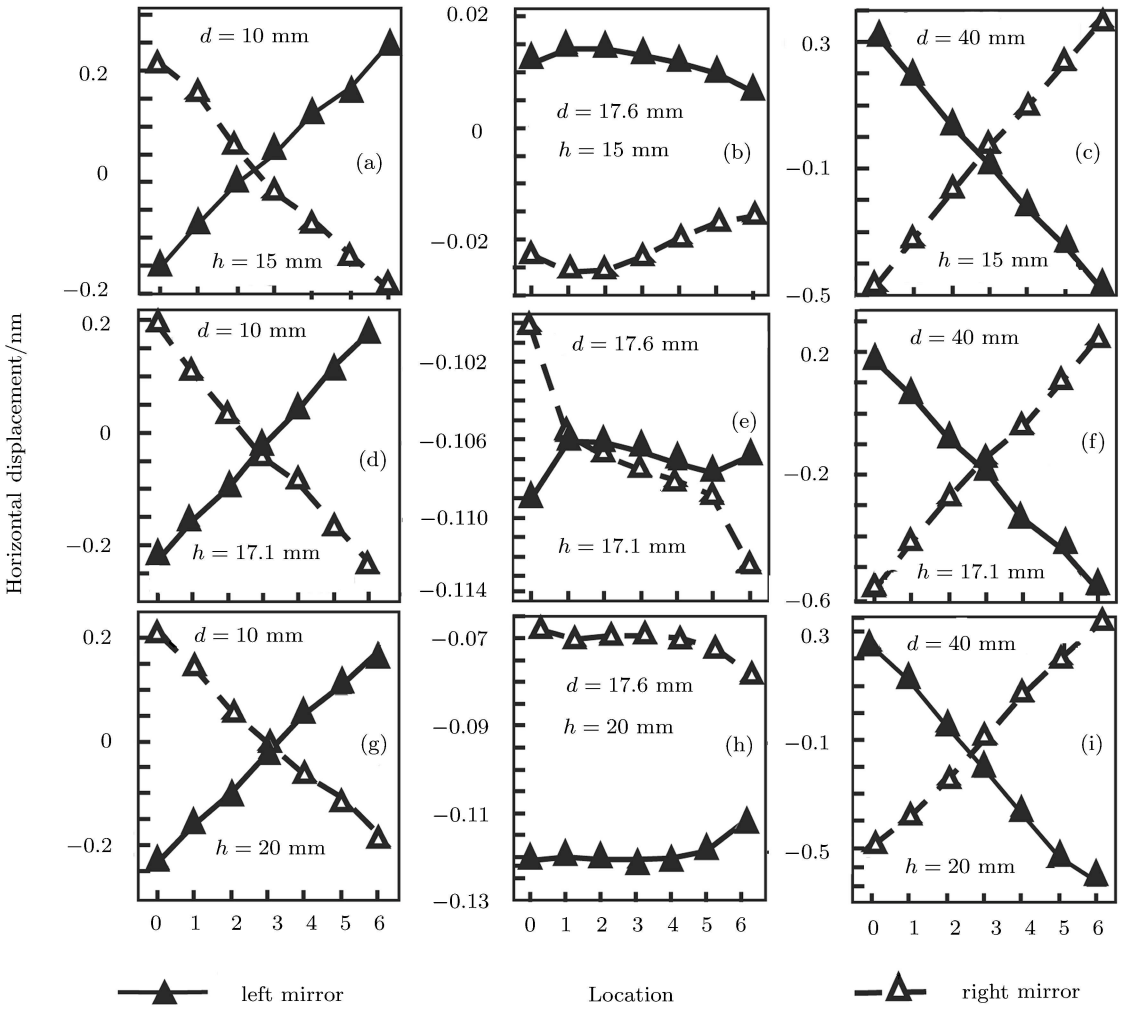


Fig.8. Mirror displacements of the cuboid cavity supported by four posts. The deformation of the cavity is reshaped by changing parameters h and d. The critical supporting position is found for a combination of $h = 17.1$ mm and $d = 17.6$ mm.

3.4. Cone-shaped cavity supported vertically

Thus far, we have analysed the elastic deformations of the cavities horizontally supported. Here we show that the critical supporting position can also be found in cavities vertically supported. Figure 9 illustrates a cone-shaped cavity vertically supported. The length of the cavity is 100 mm. The radius and the thickness of the middle flange are 60 mm and 10 mm, respectively. Here the vertical support is achieved by using three holes located on the middle flange of the cavity. In Fig.9, h and r are the depth of the holes and the distance between the optical axis and the central axis of the supporting holes, respectively.

We fix the value of r and vary h to search for a critical supporting position. Figure 10 shows the numerical results of mirror displacements at various h. The trend of the mirror deformation can be inferred from these numerical results. When r, the location of the hole, is fixed at 48 mm and a hole depth of 3 mm is used, the cavity is elongated with $\Delta L \approx 3 \times 10^{-10}$ m. As h is changed to 7 mm, ΔL is decreased to -3×10^{-10} m. The critical supporting position is found at $h = 5.1$ mm, with the corresponding length change $\Delta L < 5 \times 10^{-12}$ m, as shown in Fig.10(b).

The benefit of using this vertical cavity can be explained qualitatively. Under the influence of gravity, the upper and the lower halves of the cavity move downward by the same amount, leading to a cavity length that is insensitive to vertical accelerations. To be more accurate, the deformations of the two parts are also affected by the warps of the flange around the supporting points, a mechanism that is confirmed

by our calculation. Additionally, sizes, locations, and depths of the three holes on the flange can affect the deformation of the flange. Consequently, these three parameters, together with other parameters such as mass distribution, collectively determine the critical supporting position at which the sensitivity of the cavity length to vertical accelerations is minimized.

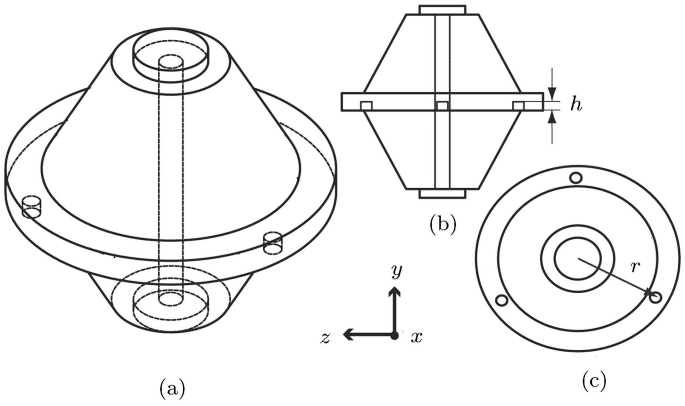


Fig.9. A cone-shaped cavity supported vertically. (a) 3D view of the cavity. (b) Side view of the cavity. (c) Top view of the cavity. The letter r stands for the distance between the optical axis and the centre of the supporting hole, h is the depth of the supporting holes. The optical axis is aligned in the direction of the gravity. The top and the bottom parts of the cavity sag in an equal amount, resulting in a cavity length that is insensitive to vertical accelerations.

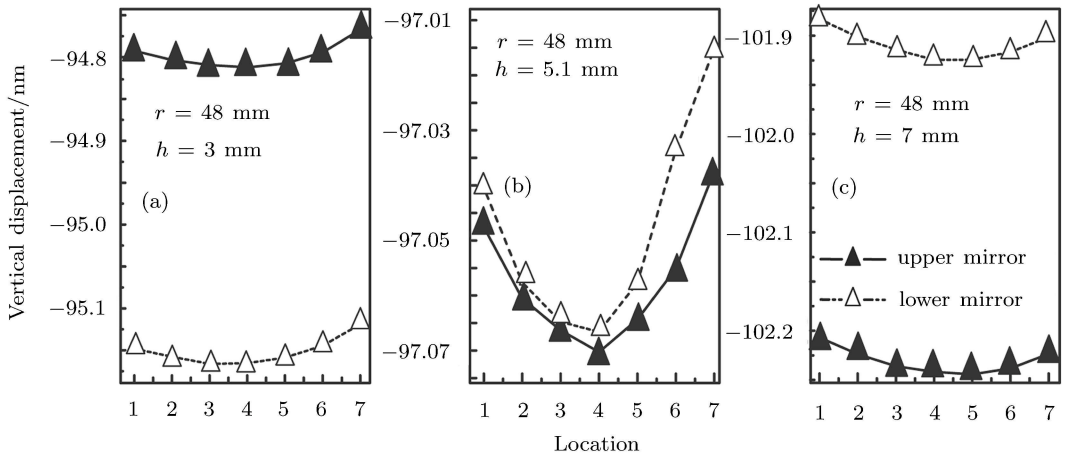


Fig.10. Mirror displacements of the cone-shaped cavity supported vertically. The length of the cavity varies with the change of the hole depth h. The critical supporting position is found at $h = 5.1$ mm when r is fixed at 48 mm.

4. The accuracy of the numerical modelling

All of the cavity designs discussed thus far are based on practical configurations used in various experiments and are analysed by FEA software. In order to apply these results to the experiment, various factors that can potentially lead to systematical errors should be considered. These factors include, but are not limited to, mesh size and constraints used in FEA, material properties of the cavity, and mechanical tolerance.

Mesh size is an important factor that can affect the precision of the numerical analysis. Indeed, a smaller mesh size will give a higher precision in the calculation. However, the smallest mesh size that can be achieved is limited by the computing resources, and a small mesh size (4−5 mm) often leads to an excessive computing time. In several numerical models, we use the mesh size that is suggested by the FEA software and subsequently use half of this size to calculate the same model. No obvious difference is observed from the two mesh sizes.

Moreover, the validity of the cavity design also

depends on an accurate modelling of the contact between the cavity and the support.

In our calculations, the example in Fig.7 shows a critical position at $d = 17.6$ mm and $h = 17.1$ mm. However, a new calculation including a modified constraint on the cavity-support interface gives the critical point at $d = 17.6$ mm and $h = 17.25$ mm. Currently, the contact between the cavity and its support is supposed to be bonded in the numerical analysis, namely there is no relative movement between the two contacting surfaces in all directions. We will further investigate this contact problem by simulating cavity-support interface with relaxed constraints.

The deviation of material properties from their nominal values should also be considered in the numerical analysis. The deformation of the cavity is directly related to the material properties such as elastic modulus, Poisson's ratio, and the mass distribution. These properties can vary among different batches and some of them are influenced by fluctuations of environmental parameters such as ambient temperatures. To evaluate the stability of the numerical models in terms of the material properties, we modify these parameters by as large as five percent. Instability of the cavity designs discussed in this paper is not observed in the calculations with the modified material properties.

In the process of the fabrication, deviations from the optimized geometrical dimensions are unfortunately always present, albeit can be lowered with increasing effort and cost. We also verify the stability of various cavity designs in terms of mechanical tolerance. For example, with a mechanical tolerance of 0.05 mm, the instability of our numerical models is not observed.

5. Summary

In this paper, we quantitatively analysed the stability of Fabry–Perot cavities using FEA. Vibration-induced elastic deformation is one of the major noise sources of Fabry–Perot cavities. Elastic deformations of Fabry–Perot cavities with various shapes and mounting configurations have been quantitatively analysed in great detail (strain distribution and mirror displacements obtained).

Four types of Fabry–Perot cavities are analysed in this paper. Firstly, widely used cylindrical cavities with horizontal mounting are analysed. In this configuration, the vertical compression of the cavity material due to gravity is coupled to the horizontal extension, resulting in an elongation of the cavity. To compensate for this coupling effect, we modelled a cuboid cavity horizontally supported by two beams, a mounting method that allows for the bending of the cavity spacer. We show that with an optimization of the width and the position of the beam, it is possible to reduce the vibration sensitivity of the cavity. Nevertheless, the benefit of this mounting method is limited in that it may not work for short cavities. Furthermore, we demonstrate that if the supporting plane of the horizontal cuboid cavities is shifted upward from the bottom then the stability of the cavity is greatly improved. Finally, we introduced an alternative mounting scheme in which the cavity is vertically supported near its midplane.[13]

Through a proper choice of the cavity geometry and the related structural support the cavity length can be protected against vibrational perturbations. In addition, the precision of numerical modelling is discussed from a computational perspective. The numerical analysis presented here provides a novel approach for the design and the construction of ultra-stable cavities. In conjunction with the traditional vibration control, the cavity geometries and mounting methods introduced here provide an economical and effective method to reduce the frequency noise of the cavity-stabilized lasers, an approach that can be applied to many experiments such as optical frequency standards, precision spectroscopy, and tests of fundamental laws of physics. Moreover, we expect that with the rapid reduction of the vibration-induced frequency noise, other noise sources such as thermal fluctuations of the cavity materials could be more easily exposed and hence investigated experimentally.

Acknowledgments

Suggestions from Li Ji-Sheng at National Institute of Metrology on the issues of precision optical fabrication are gratefully acknowledged by Chen L and Zang E. Chen L would like to thank Ma Long-Sheng, Mark Notcutt, John L. Hall, and Ye Jun for stimulating discussions.

References

[1] Drever R W P, Hall J L, Kowalski F V, Hough J, Ford G M, Munley A J and Ward H 1983 *Appl. Phys.* B **31** 97

[2] Young B C, Cruz F C, Itano W M and Bergquist J C 1999 *Phys. Rev. Lett.* **82** 3799

[3] Takamoto M, Hong F L, Higashi R and Katori H 2005 *Nature* **435** 321

[4] Zhang G Y, Song F, Feng Y and Xu J J 2000 *Acta Phys. Sin.* **49** 1495 (in Chinese)

[5] Zhang G Y, Zhang C P, Ding X, Song F, Guo S G and Meng F Z 2002 *Acta Phys. Sin.* **51** 253 (in Chinese)

[6] Chen K X, Yi M B, Zhang D M and Hou A L 2000 *Acta Phys. Sin.* **49** 1611 (in Chinese)

[7] Lu C G, Cui Y P, Wang Z Y and Yun B F 2004 *Acta Phys. Sin.* **53** 145 (in Chinese)

[8] Zhang G Y 1979 *Acta Phys. Sin.* **28** 891 (in Chinese)

[9] Zhang G Y 1991 *Acta Phys. Sin.* **40** 1065 (in Chinese)

[10] Seigman A E 1986 *Lasers* (USA: Stanford University Press) p744

[11] Bachor H A and Ralph T C 2003 *A Guide to Experiments in Quantum Optics* (Berlin: Wiley-VCH) p119

[12] Zhu M and Hall J L 1997 *Atomic, Molecular and Optical Physics: Electromagnetic Radiation* (San Diego: Academic) p103

[13] Notcutt M, Ma L S, Ye J and Hall J L 2005 *Opt. Lett.* **30** 1815